Using of artificial neural networks (ANNs) to predict the rheological behavior of magnesium oxide-water nanofluid in a different volume fraction of nanoparticles, temperatures, and shear rates

Yicheng Li[1], Rasool Kalbasi[2], Arash Karimipour[3,*], Mohsen Sharifpur[4,5], Josua Meyer[4]

[1] Automotive Engineering Research Institute, Jiangsu University, Zhenjiang, 212013, China

[2] Department of Mechanical Engineering, Najafabad Branch, Islamic Azad University, Najafabad, Iran

[3] Sustainable Management of Natural Resources and Environment Research Group, Faculty of Environment and Labour Safety, Ton Duc Thang University, Ho Chi Minh City, Vietnam

[4] Department of Mechanical and Aeronautical Engineering, University of Pretoria, Pretoria, 0002, South Africa

[5] Institute of Research and Development, Duy Tan University, Da Nang, 550000, Vietnam

*Correspondence: Arash Karimipour, Sustainable Management of Natural Resources and Environment Research Group, Faculty of Environment and Labour Safety, Ton Duc Thang University, Ho Chi Minh City, Vietnam. Email: arashkarimipour@tdtu.edu.vn

ABSTRACT

Laboratory studies are usually time-consuming and costly; hence, soft computing methodology can be an attractive alternative for predicting results. In this study, the viscosity of MgO-water nanofluid in a different volume fraction of nanoparticles, temperatures, and shear rates has been predicted by artificial neural networks (ANNs) and surface methods. In the ANN method, an algorithm is proposed to select the best neuron number for the hidden layer. In the fitting method, a surface is proposed for each volume fraction of nanoparticles, and finally, the results of the ANN and surface fitting method have been compared. It can be observed that increasing the volume fraction from 0.07% to 1.25% at temperatures of 25°C, 30°C, 40°C, 50°C, and 60°C resulted in about two-fold increase in viscosity. Also, the best network has 24 neurons in the hidden layer. It can be seen that for a network with 24 neurons in the hidden layer has the best overall correlation, and this coefficient is 0.999035. The mean absolute value of errors in the ANN and fitting method are 0.0118 and 0.0206, respectively.

KEYWORDS: artificial neural networks, MgO-water nanofluid, rheological behavior

1 INTRODUCTION

One of the concerns of different researchers is to intensifiy heat transfer in different industries to improve their performance efficiency.[1-19] Scientists have been working for years on the use of micro-fluid mixtures of very small suspended solids to improve heat transfer.[20, 21] But these fluids have had many problems, such as deposition, impurity, corrosion, and increasing pressure drop, until the idea of using nanoparticles in 1995 was first put forward by Choi[22] and the great revolution in the field of heat transfer in fluids.[23] The idea led to the creation of colloidal suspensions containing nanoparticles called nanofluids. Adding nanoparticles leads

to variations in thermal conductivity as well as viscosity.[24-34] Nanofluids have been the subject of much research because of their amazing thermal properties.

Application of nanofluids in different heat transfer cases showed that this new heat transfer fluid could improve the rate of heat transfer.[35-43] One area of nanofluid-related research that has attracted many researchers is the determination of altered fluid properties due to the presence of nanoparticles. Recent decades, artificial neural networks (ANNs) have been used in many scientific areas by researchers.[28, 44] Because of new advances in processing data, these networks have been more popular in predicting the behavior of systems, especially systems with nonlinear behavior of complex systems. Various types of computational models have been introduced as generic ANNs, each of which can be used for a variety of applications, each inspired by a particular aspect of the capabilities and properties of the human brain. Today, the use of intelligent systems, especially ANNs, has become so widespread that these tools can be categorized as basic and common tools in the form of basic mathematical operations.

Ramezanizadeh et al.[45] reviewed the utilization of machine learning approaches on predicting dynamic viscosity of nanofluids. Ahmadi et al.[46] investigated the connectionist methods to estimate the thermal conductivity of TiO_2/water nanofluid. Dalkilic et al.[47] predicted the rheological behavior of graphite/water nanofluids by means of ANNs. Longo et al.[48] applied the ANN method for modeling the rheological behavior of oxide-based nanofluids. Their model shows a fair agreement in predicting experimental data. Nasirzadehroshenin et al.[49] used Ann-GA method to model heat transfer behavior of carbon nanotube nanofluid in a tube with constant temperature at walls. Alrashed et al.[50] obtained the properties of Cu-silica/water nanofluids with the ANN method. Kahani et al.[51] applied machine learning methods to predict Nusselt number and pressure drop of TiO_2/water nanofluid in nonstraight paths. Shahsavar et al.[52] developed ANNs and measured the thermal conductivity and viscosity for liquid paraffin/Al_2O_3 nanofluid. Ahmadi et al.[53] used a smart model to predict the dynamic viscosity of SiO2/ethylene glycol/water nanofluid.

In this study, we predict the rheological behavior of MgO-water nanofluid by using experimental data and ANN method. Nanofluid with volume fraction of nanoparticles values of ϕ=0.07%, 0.14%, 0.28%, 0.42%, 0.56%, 0.76%, 1%, and 1.25% are prepared for the experiments. The temperatures studied are 25°C, 30°C, 40°C, 50°C, and 60°C. According to the authors' research, there is no investigation with ANN into the rheological behavior of MgO-water nanofluid.

2 EXPERIMENTAL DATA

In this study, the MgO/water nanofluid viscosity is predicted at 0.07, 0.14, 0.28, 0.42, 0.56, 0.76, 1, and 1.25 vol.%. In an experimental study, Khodaddi et al.[54] investigated the nanofluid viscosity. They showed that the behavior of the nanofluid is non-Newtonian, and therefore, the viscosity depends on the temperature, the volume fraction of the nanoparticles, and the shear rate. To understand the effects of shear rate on nanofluid viscosity, the authors performed viscosity measurements on shear rates in the range of 20 to 60 rpm.[54] On the other hand, the increase in temperature causes the fluid molecules to slip with less friction. This means that with increasing the temperature, the viscosity diminishes. To study the effect of temperature, the authors measured the viscosity at temperatures of 25°C, 30°C, 40°C, 50°C, and 60°C. Figure 1 shows the dynamic viscosity variations versus volume fraction of nanoparticles at different temperatures at 20 rpm.[54] It can be seen from this figure that increasing ϕ from 0.07% to 1.25% at temperatures of 25°C, 30°C, 40°C, 50°C, and 60°C resulted in about two-fold

increase in viscosity. The percentage increase is higher at higher temperatures. At $T = 60°C$, the initial inertia diagram does not contain the increase in the other diagrams and viscosity increases with almost constant slope change in all volume fractions. Higher temperatures lead to more molecular motions, and the temperature factor causes the slope of the increases to remain constant at $T = 60°C$.

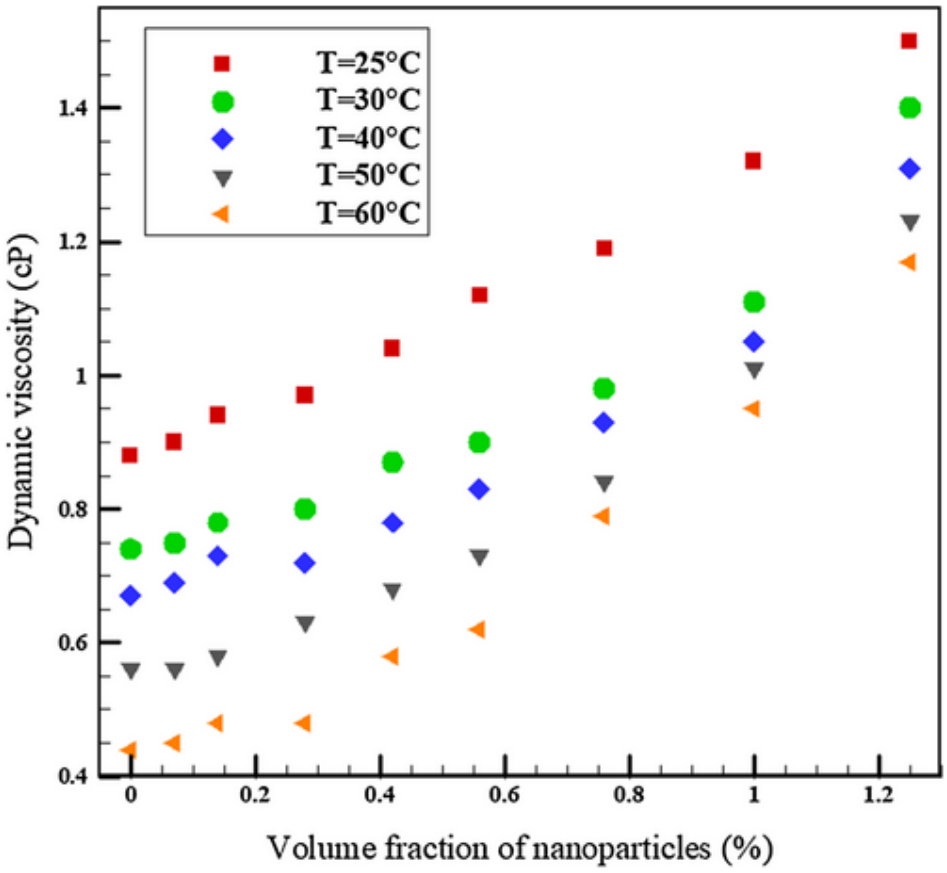

FIGURE 1. Dynamic viscosity versus volume fraction[54]

Figure 2 shows the dependency between dynamic viscosity and the shear rate at ϕ=0.14% and different temperatures. Note the apparent viscosity changes at 50% of the first round change. These large changes are due to the shear-thinning behavior that decreases with higher rotation. The effects of particle aggregation and shear-heating are not measurable and far from the researcher's point of view and should be addressed in more advanced research. After examining, it becomes clear that this behavior is observed in all nanofluid volume fractions. In other words, the water-MgO nanofluid exhibits a high shear thinning or non-Newtonian behavior in all volume fractions. However, in some cases, the slight effects of shear heating must be taken into account.

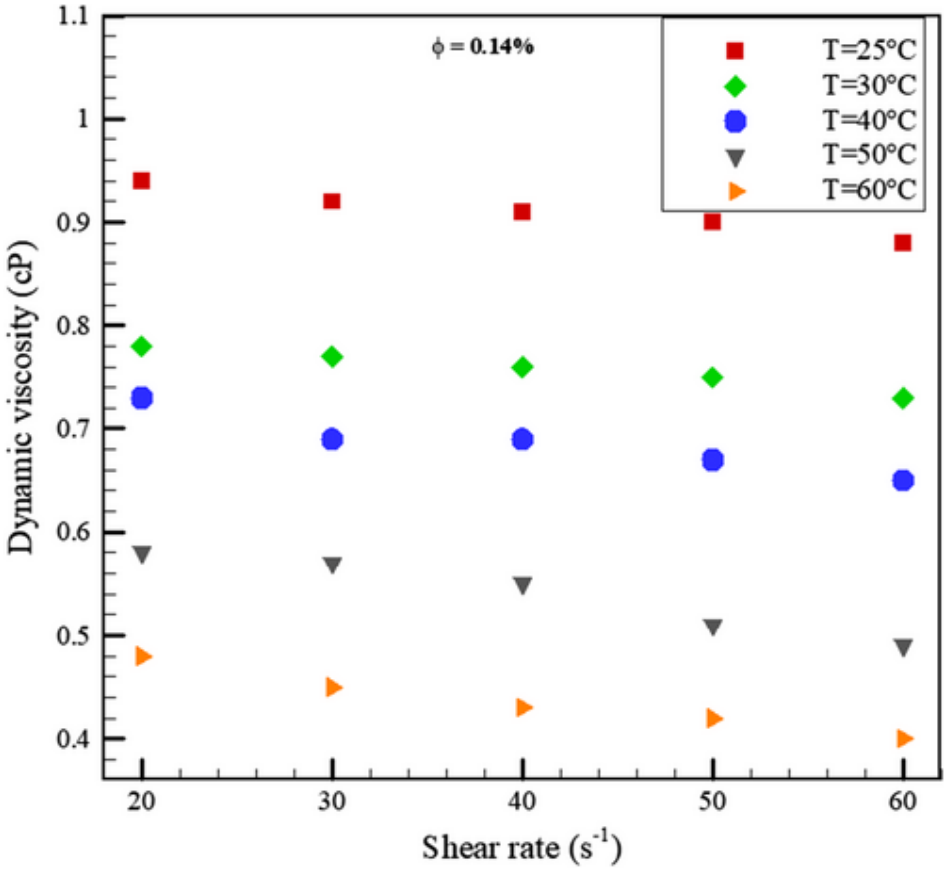

FIGURE 2. The dependency of dynamic viscosity to shear rate[54]

3 ANN METHOD

A simple model of ANN firstly was introduced by Warren McCulloch and Walter Pitts in 1943. This simple model was called threshold logic. Then, in the late 1940s, D.O. Hebb proposed a learning method, which was an unsupervised method. Frank Rosenblatt in 1958 created the perceptron, which is an algorithm based on the simplified model of a real biological neuron. Each neuron consists of weights, bias, and activation function. In Figure 3, the architecture of a single neuron has been shown.

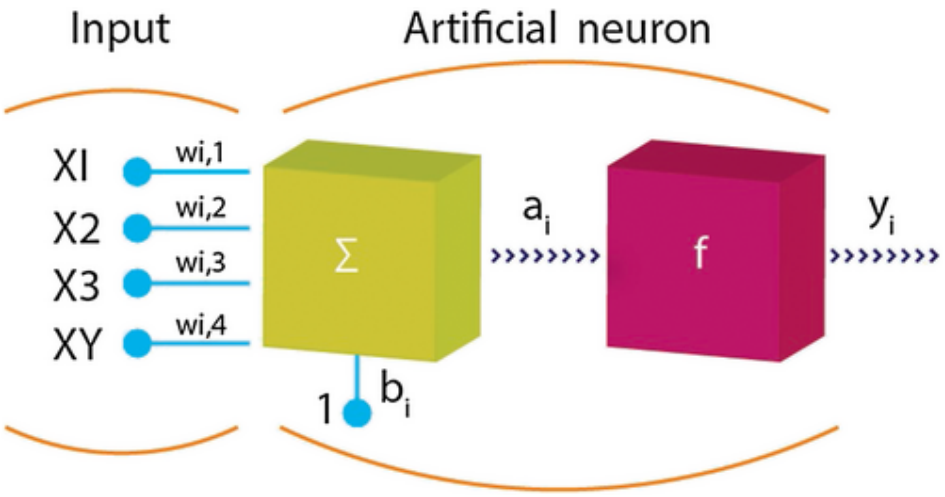

FIGURE 3. The architecture of artificial neural network (ANN)

The process of input data is presented in Equation 1[45]:

$$Y_i = \emptyset\left(\sum_{j=1}^{n} w_{ij}x_j + b_i\right) \tag{1}$$

In Equation 1, $\emptyset$ is the activation function, x_j is the jth input and b_i is the bias of the ith neuron and Y_i is the output of ANN. In the current study, the activation function of the hidden layer is tansig which is presented in Equation 2, and the activation function of the output layer is purelin,[45]

$$\tan sig\,(x) = \frac{2}{1+e^{-2x}} - 1 \tag{2}$$

In this work, the learning algorithm is Levenberq-Marquardt. This algorithm for the first time was introduced by Kenneth Levenberg in 1944, and then in 1963, it was rediscovered by Donald Marquardt. The data points are divided into three parts including train, validation, and test. In this work, 70% of data is used for training, 15% for validation, and 15% for test. The train data points are used in training the ANN, the validation is used in adjusting the training process, and the test data points are used at the final step to evaluate the performance of the network. The performance of the network is considered as mean square error (MSE) which is the average difference between the estimated values and the experimental data and is defined in Equation 3[45]

$$MSE = \frac{1}{N}\sum_{i=1}^{N}(\mu_{Pred} - \mu_{Exp}) \tag{3}$$

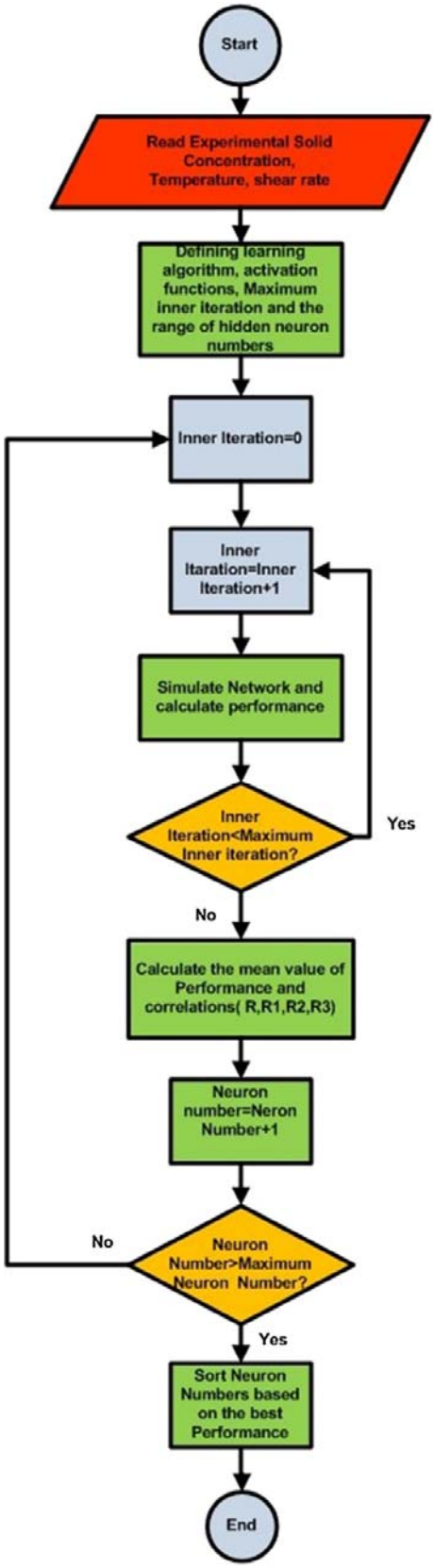

FIGURE 4. Algorithm of finding the best neuron

Obviously, in calculating the MSE, closer values to zero are better. ANNs are based on the processing data by neurons. Therefore, the number of neurons has important effects on outputs. As this ANN should predict only one parameter (viscosity); therefore, only one neuron in the output layer is used. To find the optimum ANN with the best neurons in the hidden layer, different networks have been tested. To increase the reliability of the ANN, for each specified neuron, the ANN has been rune for 20 times, and finally, the mean value of these performances has been considered as the performance for that neuron number. To find the best neuron number in the hidden layer, an algorithm has been used, which is presented in Figure 4.

The results of different neuron numbers for ANN have been presented in Table 1.

TABLE 1. The performances versus neuron number

Neuron Number	Sorted Performance	Train Performance	Validation Performance	Test Performance
24	0.000301888	0.000129534	0.000522529	0.000877058
23	0.000305033	0.00012217	0.000515833	0.000969415
14	0.000318204	0.000187376	0.000389836	0.000813219
25	0.000333332	0.000129642	0.000615607	0.001003698
28	0.000358753	0.000103909	0.000653542	0.001354837
31	0.0003609	0.000128631	0.000637951	0.001218501
17	0.000370908	0.000207881	0.000444941	0.001040071
21	0.000371807	0.000189746	0.000514374	0.001068273
19	0.000374295	0.000210131	0.000493419	0.00097527
18	0.000375719	0.000195033	0.000496417	0.001093228
15	0.000388643	0.000216797	0.000542748	0.000973666
32	0.000392071	0.000139053	0.000631341	0.001428436
30	0.00040017	0.000151	0.00074376	0.001231189
16	0.000409228	0.000253081	0.000470384	0.001007488
12	0.000413256	0.000244385	0.000516859	0.001031494
13	0.000414593	0.00025096	0.000530356	0.000973507
26	0.000441884	0.000186195	0.000677746	0.001449338
27	0.000445452	0.000213152	0.00072102	0.001214165
29	0.000447328	0.000134501	0.000961024	0.001417292
35	0.000461733	9.76257E-05	0.000881205	0.001942658
33	0.000477153	0.000149652	0.000775301	0.001870102
10	0.000487449	0.000339829	0.00043166	0.001127671
9	0.000503781	0.000364835	0.000500502	0.000978201
11	0.000507273	0.000356589	0.000536789	0.001010639
43	0.000547098	8.41851E-05	0.001249648	0.002199763
20	0.000556205	0.000279525	0.000616951	0.001875994
22	0.000601928	0.000256952	0.000546784	0.002557997
34	0.000644599	0.000135552	0.00128343	0.002631452
41	0.000689736	8.61753E-05	0.001289749	0.003380417
38	0.00072683	0.000155975	0.001213538	0.0033216
36	0.000768115	0.00011263	0.002132269	0.002518887
40	0.000984908	0.000251453	0.002354221	0.003061927
46	0.000990069	0.000321305	0.001800779	0.003491418
39	0.000991612	0.000280648	0.001863753	0.003700153
42	0.00112044	0.000367403	0.001832495	0.004255262
8	0.001216051	0.000936749	0.000917129	0.002421718
47	0.001237904	0.00040015	0.002213574	0.004438301
45	0.001353802	0.000425266	0.002554848	0.004727508

48	0.001473198	0.000326827	0.004143292	0.00393534
44	0.001650976	0.00040958	0.002796129	0.007077342
37	0.002212385	0.000603304	0.004972929	0.007106403
49	0.002289438	0.000194014	0.004317576	0.011833481
50	0.002375294	0.000452646	0.005364934	0.009012165

Considering Table 1, it can be seen that the best network has 24 neurons in the hidden layer. Although an ANN with 24 neurons in the hidden layer has acceptable performance, another criterion to judge about outputs is correlation coefficient which is presented in Equation 4. The correlation coefficient shows the compatibility between inputs and outputs and this coefficient is defined as:

$$r = \frac{\sum_{i=1}^{n} (\mu_{Exp} - \bar{\mu}_{exp})(\mu_{Pred} - \bar{\mu}_{Pred})}{\sqrt[2]{\sum_{i=1}^{n} (\mu_{Exp} - \bar{\mu}_{exp})^2} \sqrt[2]{\sum_{i=1}^{n} (\mu_{Pred} - \bar{\mu}_{Pred})^2}}, \quad (4)$$

where $\bar{\mu}_{exp}$ and $\bar{\mu}_{Pred}$ are the mean value of the experimental and predicted data, respectively.

In Table 2, the correlation of data outputs including train, validation, test and all ANN outputs has been presented.

TABLE 2. Artificial neural network **(**ANN) correlation coefficient outputs

Neuron Number	Train Correlation	Validation Correlation	Test Correlation	All Correlation
24	0.999518144	0.997963857	0.997417985	0.999035782
23	0.999520473	0.997921442	0.997933915	0.999028849
14	0.999267819	0.998454917	0.998193525	0.998981013
25	0.999513346	0.997022224	0.997553928	0.998932573
28	0.999590869	0.997625899	0.997310754	0.998862462
31	0.999520932	0.997766287	0.996233139	0.998845966
17	0.999236485	0.99823857	0.997827802	0.99882444
21	0.999319002	0.997825204	0.996740544	0.998803659
19	0.99924926	0.99801026	0.997620982	0.998814216
18	0.999278395	0.998106528	0.997489304	0.998806524
15	0.999186779	0.997976292	0.997427146	0.998754239
32	0.999488141	0.997485566	0.996167116	0.998746495
30	0.999447289	0.996860002	0.996783132	0.998724038
16	0.999076432	0.99798066	0.996911201	0.99866855
12	0.999048559	0.998290593	0.997754508	0.998675
13	0.999056183	0.997713984	0.997967071	0.99866651
26	0.999327534	0.997013095	0.996225976	0.998593965
27	0.999259574	0.997654485	0.996273957	0.998593794
29	0.999459292	0.996792971	0.996041012	0.998554597
35	0.999630409	0.996564925	0.995857541	0.998513712
33	0.999482379	0.997142283	0.995213226	0.998507102
10	0.998645957	0.998092186	0.99761496	0.998422737
9	0.99860441	0.997824957	0.997632541	0.998368443
11	0.9985841	0.998139548	0.997791856	0.998371153
43	0.999694541	0.994794734	0.994493927	0.998247949
20	0.999067584	0.99751348	0.995293872	0.998373194
22	0.998967836	0.997468039	0.996522077	0.998201793

34	0.99949969	0.995225749	0.995120072	0.998030975
41	0.999682734	0.996406752	0.992743343	0.997812274
38	0.999396285	0.994993638	0.993957525	0.997694522
36	0.999583973	0.991936012	0.993642827	0.997551472
40	0.999115588	0.99228154	0.993049263	0.996878132
46	0.998883634	0.993638119	0.991615235	0.996937781
39	0.998996152	0.992812045	0.990555341	0.996821294
42	0.998708521	0.991688759	0.989196325	0.996409144
8	0.996786834	0.996495971	0.993773918	0.996076518
47	0.998512041	0.99104953	0.987959378	0.99600853
45	0.99807263	0.989900427	0.989185977	0.995647482
48	0.998829551	0.98760951	0.987296927	0.995274055
44	0.998451667	0.987932526	0.986041219	0.994674204
37	0.997199774	0.982049345	0.989051105	0.992763244
49	0.999471697	0.983537055	0.974933815	0.992731006
50	0.998744568	0.9785739	0.97844572	0.992569362

It can be seen that for a network with 24 neurons in the hidden layer has the best overall correlation, and this coefficient is 0.999035. In Figures 5-8, the train, validation, test, and all outputs of ANN have been depicted. Figure 5 shows the training output of ANN versus target. In this ANN, the MSE and maximum absolute value of error for train data are 1.2954e-04 and 0.0345, respectively.

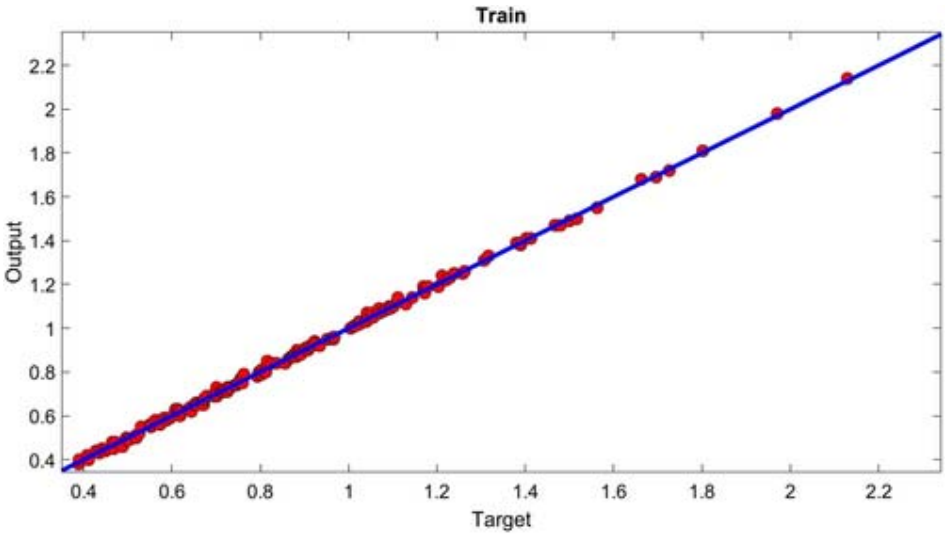

FIGURE 5. The training output of artificial neural network (ANN)

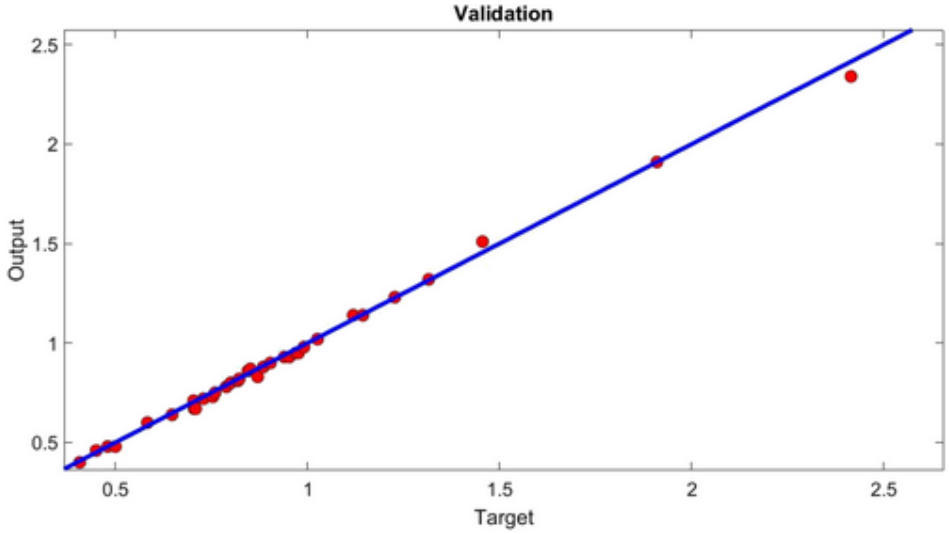

FIGURE 6. The validation output of artificial neural network (ANN)

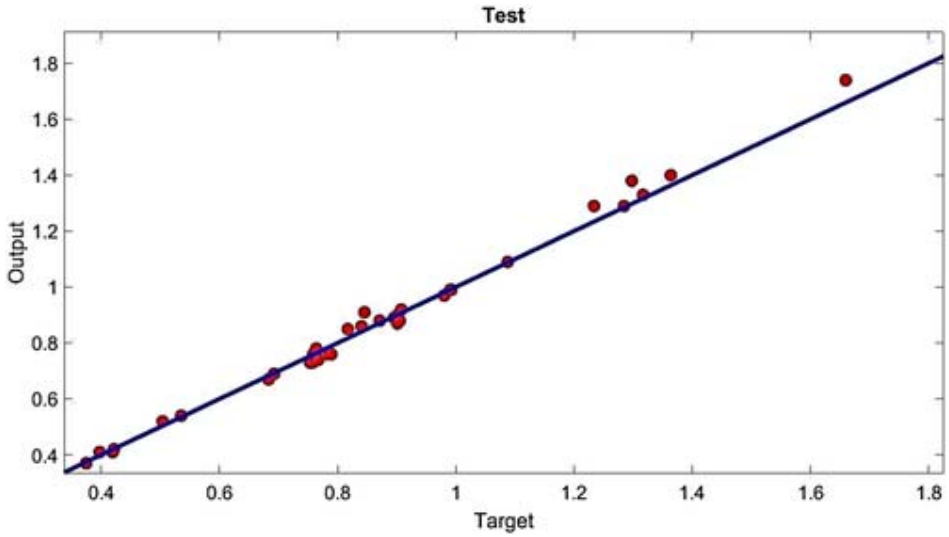

FIGURE 7. The test output of artificial neural network (ANN)

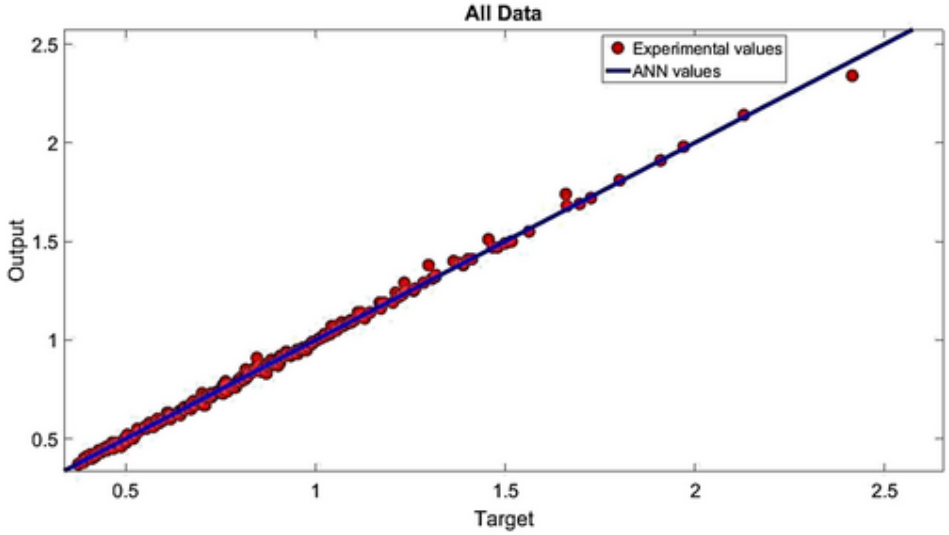

FIGURE 8. All outputs of artificial neural network (ANN)

Figure 6 shows the validation output of ANN. In this ANN, the MSE and maximum absolute value of error for validation data are 5.2252e-04 and 0.0748, respectively.

Figure 7 shows the test output of ANN. In this ANN, the MSE and maximum absolute value of error for test data are 8.7705e-04 and 0.0822, respectively.

Figure 8 shows all outputs of ANN. In this ANN, the MSE and maximum absolute value of error for all data are 3.0188e-04 and 0.0822, respectively.

4 SURFACE FITTING

Considering data points, there are three inputs including ϕ, temperature, shear rate, and one target (dynamic viscosity). As there are eight volume fraction of nanoparticles, for each volume fraction, a surface is fitted based on the temperature and shear rate. The fitted surfaces for all volume fraction of nanoparticles are presented in Figures 9-17.

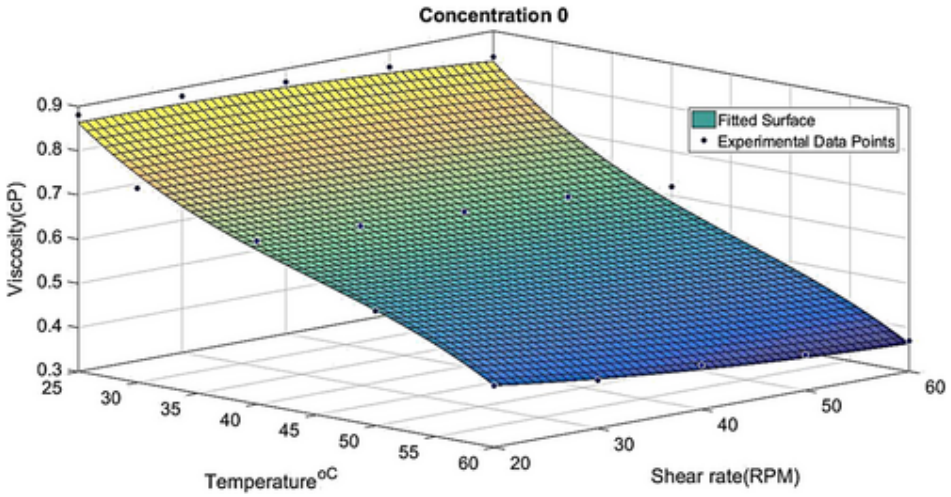

FIGURE 9. The fitted surface for ϕ=0%

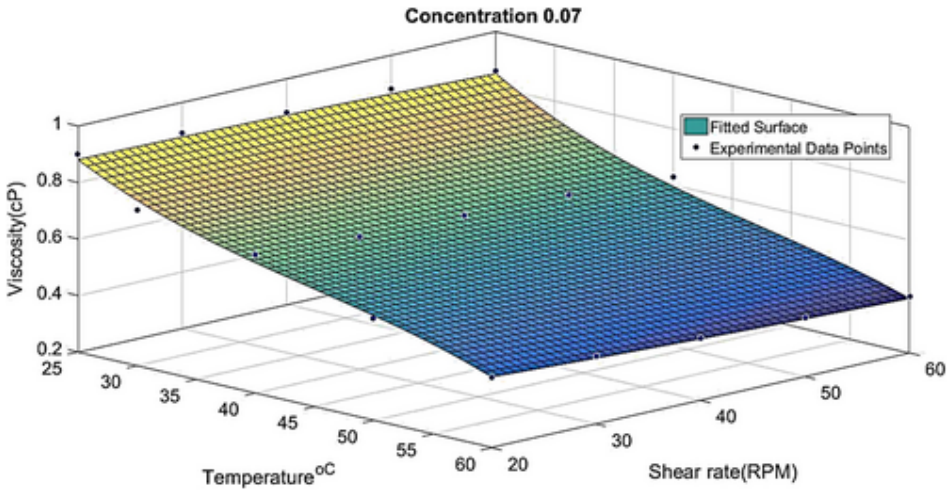

FIGURE 10. The fitted surface for ϕ=0.07%

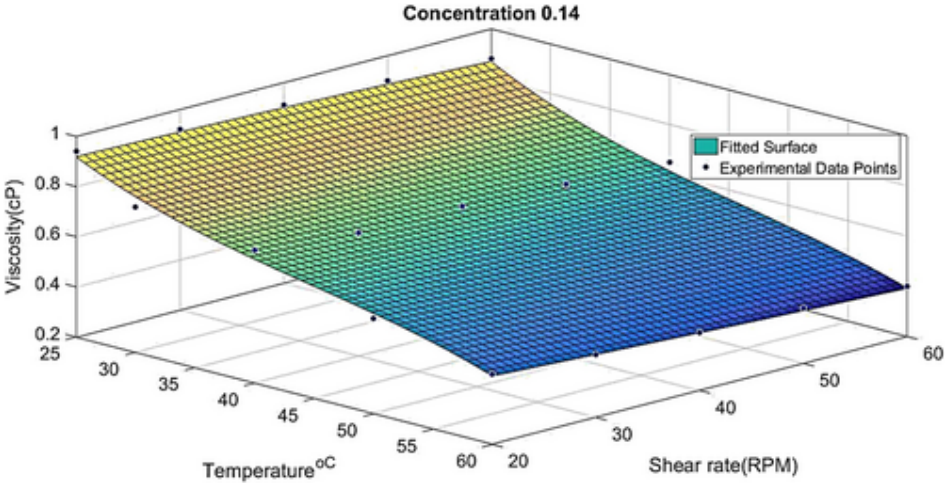

FIGURE 11. The fitted surface for ϕ=0.14%

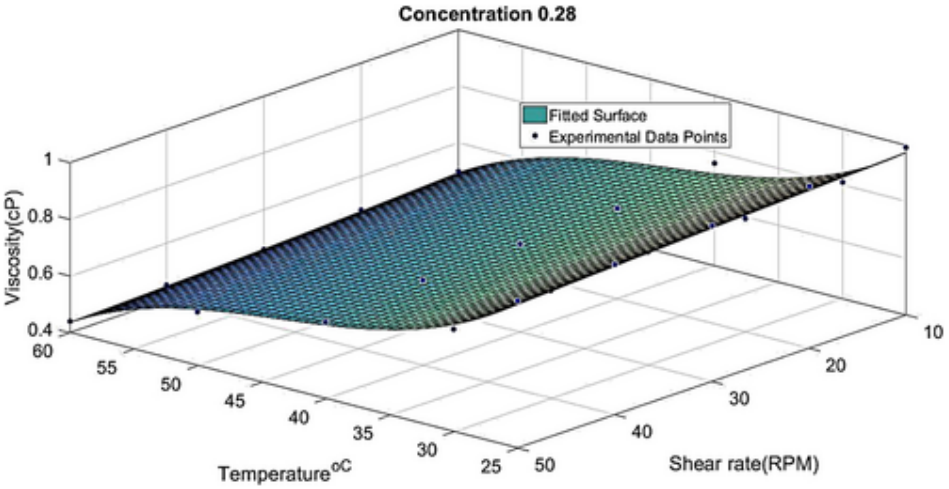

FIGURE 12. The fitted surface for ϕ=0.28%

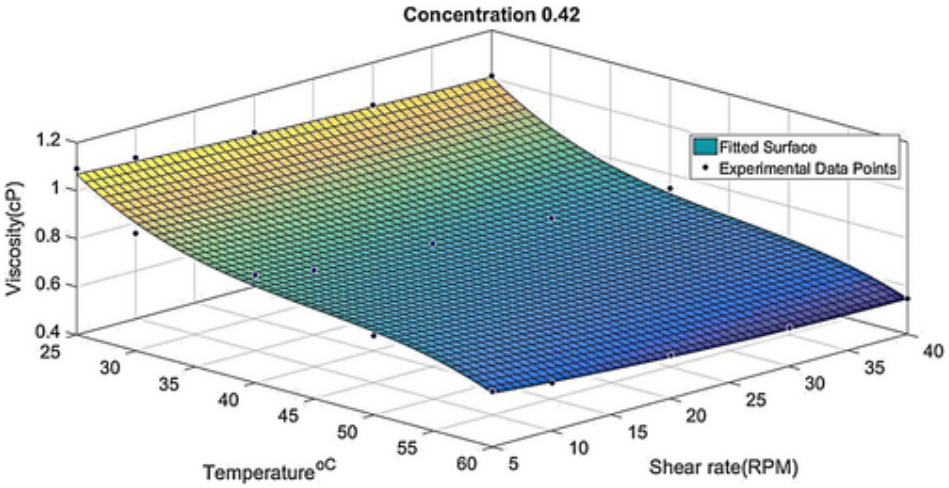

FIGURE 13. The fitted surface for ϕ=0.42%

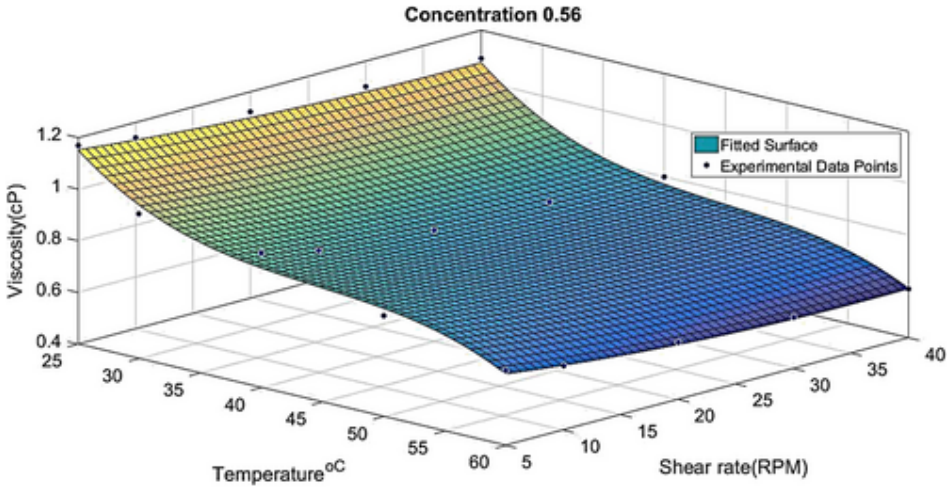

FIGURE 14. The fitted surface for ϕ=0.56%

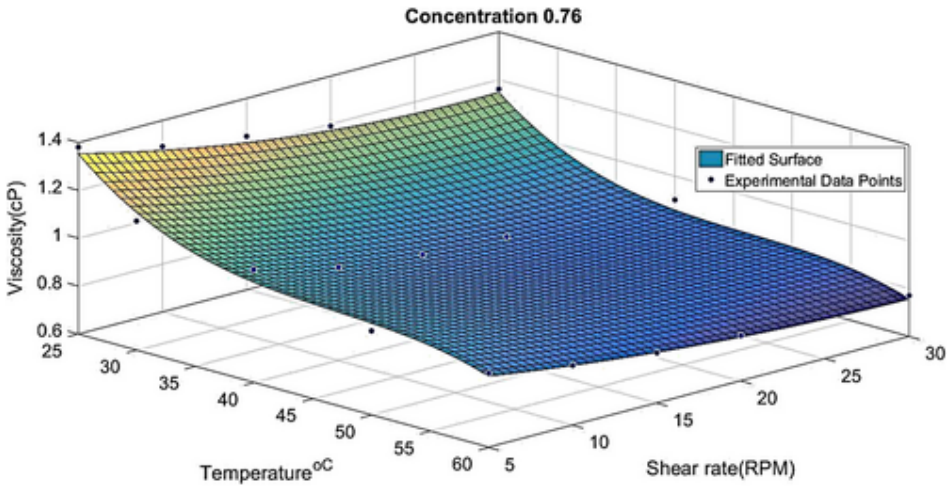

FIGURE 15. The fitted surface for ϕ=0.76%

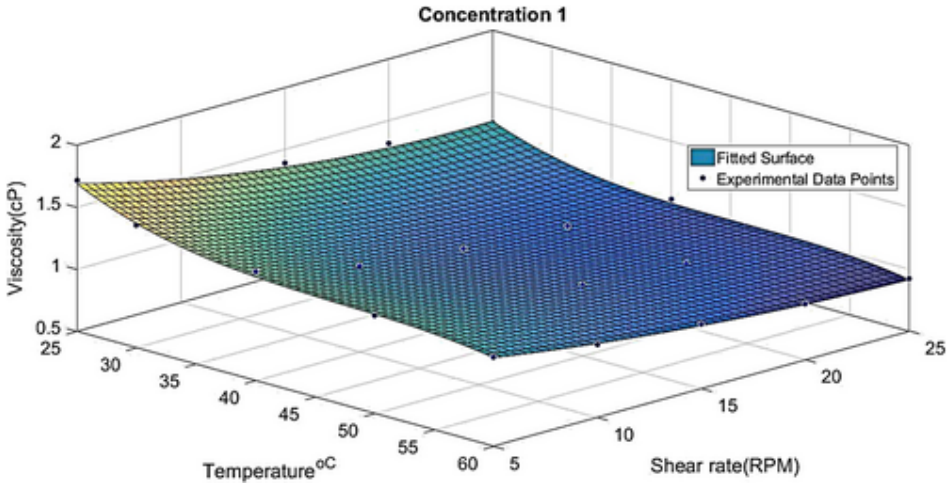

FIGURE 16. The fitted surface for ϕ=1

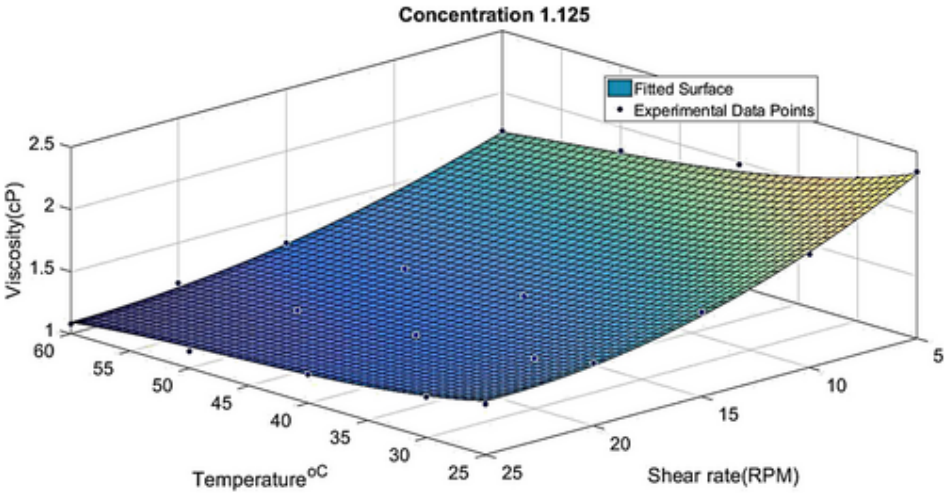

FIGURE 17. The fitted surface for ϕ=1.125%

For the temperature, a third-order polynomial and for the shear rate, a second-order polynomial is proposed. It should be mentioned that different orders for temperature and shear rate have been tested, and these orders showed the best results. The general format of the fitted surface is shown in Equation 5,

$$\mathbf{fitresult(x,y) = p00 + p10{*}x + p01{*}y + p20{*}x^2 + p11{*}x{*}y + p02{*}y^2 + p30{*}x^3 + p21{*}x} \quad (5)$$

In Equation 5, x and y representing temperature and representing the shear rate, respectively. As mentioned before, for each volume fraction of nanoparticles a surface is fitted. The coefficients of these fitted surfaces are presented in Table 3.

TABLE 3. The coefficients of fitted surface for different concentrations

	p00	**p10**	**p01**	**p20**	**p11**	**p02**	**p30**	**p21**	**p12**
0	1.87711 4078	−0.07078 1998	0.006771 797	0.00145 9169	−0.00024 3987	−6.61E-05	−1.10E-05	1.02 E-06	1.58 E-06
0.07	1.92449 3578	−0.07082 8035	0.005071 355	0.00143 4677	−0.00024 0395	−3.04E-05	−1.09E-05	1.98 E-06	6.71 E-07
0.14	2.02657 3855	−0.07431 1808	0.003325 847	0.00149 6984	−0.00017 3161	−2.68E-05	−1.13E-05	1.27 E-06	5.49 E-07
0.28	3.14848 2846	−0.15694 4354	−0.00037 4448	0.00348 7513	−4.15E-05	−1.79E-05	−2.67E-05	1.87 E-07	5.05 E-07
0.42	3.17657 6564	−0.14870 6373	−0.00018 856	0.00319 0438	−0.00015 9029	1.18E-05	−2.36E-05	1.33 E-06	8.43 E-07
0.56	3.79432 005	−0.18934 1556	−0.00280 2818	0.00416 1837	−0.00012 3257	4.88E-05	−3.11E-05	9.99 E-07	7.22 E-07

0.76	4.255124575	−0.196324519	−0.031639255	0.004090283	0.000462285	0.000511193	−2.89E-05	−2.38E-06	−5.25E-06
1	4.938722199	−0.20718094	−0.084176289	0.004242534	0.001229759	0.00165	−2.97E-05	−5.92E-06	−1.82E-05
1.125	4.916984114	−0.12741697	−0.161843594	0.00208414	0.002215439	0.002985714	−1.28E-05	−1.14E-05	−2.72E-05

In Figure 18, the ANN and fitting absolute value of errors have been shown. It can be observed that the ANN has smaller absolute values of errors. The mean absolute value of errors in ANN and fitting method are 0.0118 and 0.0206, respectively. Also, the correlation coefficient between inputs and ANN outputs is and the correlation with each other.

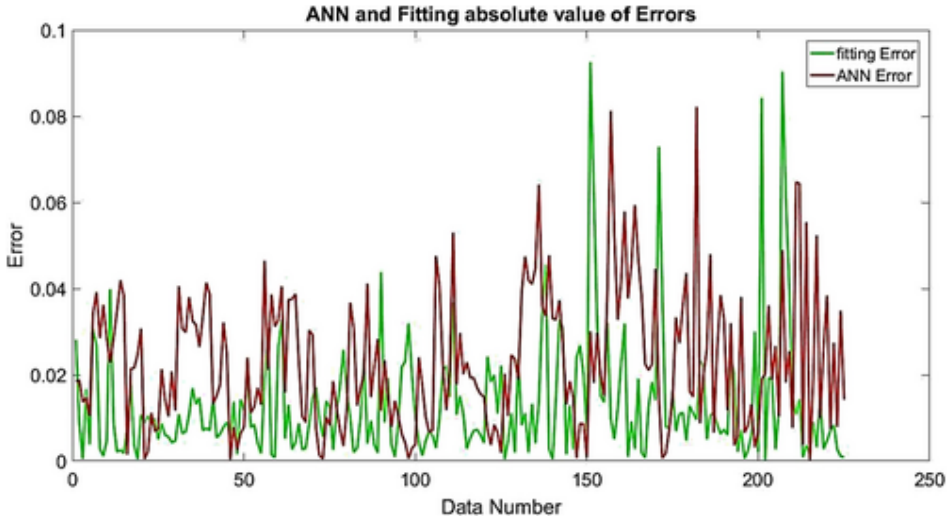

FIGURE 18. Absolute value of errors in artificial neural network (ANN) and fitting method]

5 CONCLUSION

In this study, an algorithm is presented to find the optimum ANN is presented to predict the viscosity of MgO-water nanofluid. Also, a surface fitting method has been used, and the correlation coefficient between experimental data and of ANN outputs and also between experimental data and surface fitting method has been applied. It can be seen that the ANN had better results compared with the fitting method.

- Increasing the ϕ from 0.07% to 1.25% at temperatures of 25°C, 30°C, 40°C, 50°C, and 60°C resulted in about two-fold increase in viscosity.
- The best network has 24 neurons in the hidden layer.
- An ANN with 24 neurons in the hidden layer has the best overall correlation, and this coefficient is 0.999035.
- The mean absolute value of errors in ANN and fitting method are 0.0118 and 0.0206, respectively.

Given the accuracy of the developed neural network, this method can also be used to estimate the viscosity of other nanoparticles.

ACKNOWLEDGEMENTS

The work is supported by China Postdoctoral Science Foundation (2018M642181), National Natural Science Foundation of China (no. 51679181, U1764262), and the National Key Research and Development Program of China (2017YFB0102603). Also, the authors declare no conflict of interest.

NOMENCLATURE SYMBOLS

ANN	Artificial neural network
b	Bias (Equation 1)
MSE	Mean square error
n	Number of data (Equation 3)
w	Weight (Equation 1)
x	Input (Equation 1)
y	Output (Equation 1)
Y	Actual value (Equation 3)
$\hat{Y}$	Predicted value (Equation 3)

GREEK LETTERS

ϕ	Volume fraction
σ	Standard deviation
μ	Mean value
Ø	Activation function (Equation 1)

REFERENCES

1. Afrand M. Using a magnetic field to reduce natural convection in a vertical cylindrical annulus. *Int J Thermal Sci*. 2017; 118: 12-23.
2. Karimi A, Afrand M. Numerical study on thermal performance of an air-cooled heat exchanger: effects of hybrid nanofluid, pipe arrangement and cross section. *Energ Conver Manage*. 2018; 164: 615-628.
3. Parsa SM, Rahbar A, Koleini M, Aberoumand S, Afrand M, Amidpour M. A renewable energy-driven thermoelectric-utilized solar still with external condenser loaded by silver/nanofluid for simultaneously water disinfection and desalination. *Desalination*. 2020; 480: 114354.
4. Pordanjani AH, Jahanbakhshi A, Nadooshan AA, Afrand M. Effect of two isothermal obstacles on the natural convection of nanofluid in the presence of magnetic field

inside an enclosure with sinusoidal wall temperature distribution. *Int J Heat Mass Transf*. 2018; 121: 565-578.
5. S-R, Sedeh S, Toghraie D, Afrand M, Foong LK. Analysis and manegement of laminar blood flow inside a cerebral blood vessel using a finite volume software program for biomedical engineering. *Comput Methods Programs Biomed*. 2020; 190: 105384. https://doi.org/10.1016/j.cmpb.2020.105384
6. Liu W, Kalbasi R, Afrand M. Solutions for enhancement of energy and exergy efficiencies in air handling units. *J Clean Prod*. 2020; 257: 120565. https://doi.org/10.1016/j.jclepro.2020.120565
7. Kalbasi R, Izadi F, Talebizadehsardari P. Improving performance of AHU using exhaust air potential by applying exergy analysis. *J Thermal Anal Calorim*, 2020/01/20. 2020; 139(4): 2913-2923. https://doi.org/10.1007/s10973-019-09198-1
8. Yari M, Kalbasi R, Talebizadehsardari P. Energetic-exergetic analysis of an air handling unit to reduce energy consumption by a novel creative idea. *Int J Numer Methods Heat Fluid Flow*. 2019; 29: 3959-3975.
9. Shanazari E, Kalbasi R. Improving performance of an inverted absorber multi-effect solar still by applying exergy analysis. *Appl Therm Eng*. 2018; 143: 1-10.
10. Menni Y, Azzi A, Chamkha A. The solar air channels: comparative analysis, introduction of arc-shaped fins to improve the thermal transfer. *J Appl Comput Mech*. 2019; 5(4): 616-626.
11. Menni Y, Azzi A, Chamkha AJ. Computational thermal analysis of turbulent forced-convection flow in an air channel with a flat rectangular fin and downstream v-shaped baffle. *Heat Transf Res*. 2019; 50(18): 1781-1818.
12. Menni Y, Azzi A, Chamkha AJ, Harmand S. Analysis of fluid dynamics and heat transfer in a rectangular duct with staggered baffles. *J Appl Comput Mech*. 2019; 5(2): 231-248.
13. Menni Y, Chamkha A, Azzi A, Zidani C, Benyoucef B. Study of air flow around flat and arc-shaped baffles in shell-and-tube heat exchangers. *Math Model Eng Prob*. 2019; 6(1): 77-84.
14. Menni Y, Chamkha A, Zidani C, Benyoucef B. Heat and nanofluid transfer through baffled channels in different outlet models. *Math Model Eng Probl*. 2019; 6(1): 21-28.
15. Menni Y, Chamkha A, Zidani C, Benyoucef B. Numerical analysis of heat and nanofluid mass transfer in a channel with detached and attached baffle plates. *Math Model Eng Probl*. 2019; 6: 52-60.
16. Menni Y, Chamkha AJ, Azzi A. Fluid flow and heat transfer over staggered '+'shaped obstacles. *J Appl Comput Mech*. 2018. https://doi.org/10.1016/22055/jacm.2018.26277.1316
17. Menni Y, Chamkha AJ, Azzi A. Nanofluid flow in complex geometries—a review. *J Nanofluids*. 2019; 8(5): 893-916.
18. Menni Y, Chamkha AJ, Lorenzini G, Kaid N, Ameur H, Bensafi M. Advances of nanofluids in solar collectors—a review of numerical studies advances of nanofluids in solar collectors—a review of numerical studies. *Math Model Eng Probl*. 2019; 6(3): 415-427.
19. Menni Y, Chamkha AJ, Massarotti N, Ameur H, Kaid N, Bensafi M. Hydrodynamic and thermal analysis of water, ethylene glycol and water-ethylene glycol as base fluids dispersed by aluminum oxide nano-sized solid particles. *Int J Numer Methods Heat Fluid Flow*. 2020.
20. Sadeghzadeh M, Ahmadi MH, Kahani M, Sakhaeinia H, Chaji H, Chen L. Smart modeling by using artificial intelligent techniques on thermal performance of flat-

plate solar collector using nanofluid. *Energy Sci Eng*. 2019; 7(5): 1649-1658. https://doi.org/10.1002/ese3.381
21. Nazari MA, Ahmadi MH, Sadeghzadeh M, Shafii MB, Goodarzi M. A review on application of nanofluid in various types of heat pipes. *J Cent South Univ*. 2019; 26(5): 1021-1041. https://doi.org/10.1007/s11771-019-4068-9
22. Aybar HŞ, Sharifpur M, Azizian MR, Mehrabi M, Meyer JP. A review of thermal conductivity models for nanofluids. *Heat Transf Eng*. 2015; 36: 1085-1110. https://doi.org/10.1080/01457632.2015.987586
23. Maddah H, Aghayari R, Mirzaee M, Ahmadi MH, Sadeghzadeh M, Chamkha AJ. Factorial experimental design for the thermal performance of a double pipe heat exchanger using Al2O3-TiO2hybrid nanofluid. *Int Commun Heat Mass Transf*. 2018; 97: 92-102. https://doi.org/10.1016/j.icheatmasstransfer.2018.07.002
24. Afrand M. Experimental study on thermal conductivity of ethylene glycol containing hybrid nano-additives and development of a new correlation. *Appl Therm Eng*. 2017; 110: 1111-1119.
25. Dijvejin ZA, Ghaffarkhah A, Sadeghnejad S, Sefti MV. Effect of silica nanoparticle size on the mechanical strength and wellbore plugging performance of SPAM/chromium (III) acetate nanocomposite gels. *Polym J*. 2019; 51(7): 693-707.
26. Esfe MH, Rostamian H, Esfandeh S, Afrand M. Modeling and prediction of rheological behavior of Al2O3-MWCNT/5W50 hybrid nano-lubricant by artificial neural network using experimental data. *Phys A Stat Mech Appl*. 2018; 510: 625-634.
27. Ghaffarkhah A, Afrand M, Talebkeikhah M, et al. On evaluation of thermophysical properties of transformer oil-based nanofluids: a comprehensive modeling and experimental study. *J Mol Liq*. 2020; 300: 112249.
28. Keyvani M, Afrand M, Toghraie D, Reiszadeh M. An experimental study on the thermal conductivity of cerium oxide/ethylene glycol nanofluid: developing a new correlation. *J Mol Liq*. 2018; 266: 211-217.
29. Moradikazerouni A, Hajizadeh A, Safaei MR, Afrand M, Yarmand H, Zulkifli NWBM. Assessment of thermal conductivity enhancement of nano-antifreeze containing single-walled carbon nanotubes: optimal artificial neural network and curve-fitting. *Phys A Stat Mech Appl*. 2019; 521: 138-145.
30. Nadooshan AA, Esfe MH, Afrand M. Evaluation of rheological behavior of 10W40 lubricant containing hybrid nano-material by measuring dynamic viscosity. *Physica E*. 2017; 92: 47-54.
31. Nadooshan AA, Eshgarf H, Afrand M. Measuring the viscosity of Fe3O4-MWCNTs/EG hybrid nanofluid for evaluation of thermal efficiency: Newtonian and non-Newtonian behavior. *J Mol Liq*. 2018; 253: 169-177.
32. Ranjbarzadeh R, Moradikazerouni A, Bakhtiari R, Asadi A, Afrand M. An experimental study on stability and thermal conductivity of water/silica nanofluid: eco-friendly production of nanoparticles. *J Clean Prod*. 2019; 206: 1089-1100.
33. Shahsavani E, Afrand M, Kalbasi R. Experimental study on rheological behavior of water–ethylene glycol mixture in the presence of functionalized multi-walled carbon nanotubes. *J Thermal Anal Calorim*. 2018; 131(2): 1177-1185.
34. Shahsavani E, Afrand M, Kalbasi R. Using experimental data to estimate the heat transfer and pressure drop of non-Newtonian nanofluid flow through a circular tube: applicable for use in heat exchangers. *Appl Therm Eng*. 2018; 129: 1573-1581.
35. Sadeghi HM, Babayan M, Chamkha A. Investigation of using multi-layer PCMs in the tubular heat exchanger with periodic heat transfer boundary condition. *Int J Heat Mass Transf*. 2020; 147: 118970. https://doi.org/10.1016/J.IJHEATMASSTRANSFER.2019.118970

36. Tayebi T, Chamkha AJ, Djezzar M. Natural convection of CNT-water nanofluid in an annular space between confocal elliptic cylinders with constant heat flux on inner wall. *Sci Iran*. 2019; 26: 2770-2783. https://doi.org/10.24200/sci.2018.21069
37. Mansoury D, Doshmanziari FI, Kiani A, Chamkha AJ, Sharifpur M. Heat transfer and flow characteristics of Al2O3/water nanofluid in various heat exchangers: experiments on counter flow. *Heat Transf Eng*. 2020; 41: 220-234. https://doi.org/10.1080/01457632.2018.1528051
38. Alsabery AI, Mohebbi R, Chamkha AJ, Hashim I. Impacts of magnetic field and non-homogeneous nanofluid model on convective heat transfer and entropy generation in a cavity with heated trapezoidal body. *J Therm Anal Calorim*. 2019; 138(2): 1371-1394. https://doi.org/10.1007/s10973-019-08249-x
39. Rejvani M, Saedodin S, Vahedi SM, Wongwises S, Chamkha AJ. Experimental investigation of hybrid nano-lubricant for rheological and thermal engineering applications. *J Therm Anal Calorim*. 2019; 138(2): 1823-1839. https://doi.org/10.1007/s10973-019-08225-5
40. Ghalambaz M, Doostani A, Izadpanahi E, Chamkha AJ. Conjugate natural convection flow of Ag–MgO/water hybrid nanofluid in a square cavity. *J Therm Anal Calorim*. 2020; 139(3): 2321-2336. https://doi.org/10.1007/s10973-019-08617-7
41. Dogonchi AS, Tayebi T, Chamkha AJ, Ganji DD. Natural convection analysis in a square enclosure with a wavy circular heater under magnetic field and nanoparticles. *J Therm Anal Calorim*. 2020; 139(1): 661-671. https://doi.org/10.1007/s10973-019-08408-0
42. Hashemi-Tilehnoee M, Dogonchi AS, Seyyedi SM, Chamkha AJ, Ganji DD. Magnetohydrodynamic natural convection and entropy generation analyses inside a nanofluid-filled incinerator-shaped porous cavity with wavy heater block. *J Therm Anal Calorim*. 2020; 1-13. https://doi.org/10.1007/s10973-019-09220-6
43. Osman S, Sharifpur M, Meyer JP. Experimental investigation of convection heat transfer in the transition flow regime of aluminium oxide-water nanofluids in a rectangular channel. *Int J Heat Mass Transf*. 2019; 133: 895-902. https://doi.org/10.1016/j.ijheatmasstransfer.2018.12.169
44. Afrand M, Nazari Najafabadi K, Sina N, et al. Prediction of dynamic viscosity of a hybrid nano-lubricant by an optimal artificial neural network. *Int Commun Heat Mass Transf*. 2016; 76: 209-214. https://doi.org/10.1016/j.icheatmasstransfer.2016.05.023
45. Ramezanizadeh M, Ahmadi MH, Nazari MA, Sadeghzadeh M, Chen L. A review on the utilized machine learning approaches for modeling the dynamic viscosity of nanofluids. *Renew Sustain Energy Rev*. 2019; 114: 109345. https://doi.org/10.1016/J.RSER.2019.109345
46. Ahmadi MH, Baghban A, Sadeghzadeh M, Hadipoor M, Ghazvini M. Evolving connectionist approaches to compute thermal conductivity of TiO2/water nanofluid. *Phys A Stat Mech Appl*. 2020;122489. https://doi.org/10.1016/J.PHYSA.2019.122489
47. Dalkilic AS, Çebi A, Celen A, et al. Prediction of graphite nanofluids' dynamic viscosity by means of artificial neural networks. *Int Commun Heat Mass Transf*. 2016; 73: 33-42. https://doi.org/10.1016/j.icheatmasstransfer.2016.02.010
48. Longo GA, Zilio C, Ortombina L, Zigliotto M. Application of artificial neural network (ANN) for modeling oxide-based nanofluids dynamic viscosity. *Int Commun Heat Mass Transf*. 2017; 83: 8-14. https://doi.org/10.1016/J.ICHEATMASSTRANSFER.2017.03.003
49. Nasirzadehroshenin F, Sadeghzadeh M, Khadang A, et al. Modeling of heat transfer performance of carbon nanotube nanofluid in a tube with fixed wall temperature by

using ANN-GA. *Eur Phys J Plus*. 2020; 135: 217. https://doi.org/10.1140/epjp/s13360-020-00208-y
50. Alrashed AA, Karimipour A, Bagherzadeh SA, Safaei MR, Afrand M. Electro-and thermophysical properties of water-based nanofluids containing copper ferrite nanoparticles coated with silica: experimental data, modeling through enhanced ANN and curve fitting. *Int J Heat Mass Transf*. 2018; 127: 925-935.
51. Kahani M, Ahmadi MH, Tatar A, Sadeghzadeh M. Development of multilayer perceptron artificial neural network (MLP-ANN) and least square support vector machine (LSSVM) models to predict Nusselt number and pressure drop of TiO $_2$/water nanofluid flows through non-straight pathways. *Numer Heat Transf Part A Appl*. 2018; 74: 1190-1206. https://doi.org/10.1080/10407782.2018.1523597
52. Shahsavar A, Khanmohammadi S, Toghraie D, Salihepour H. Experimental investigation and develop ANNs by introducing the suitable architectures and training algorithms supported by sensitivity analysis: measure thermal conductivity and viscosity for liquid paraffin based nanofluid containing Al2O3 nanoparticles. *J Mol Liq*. 2019; 276: 850-860. https://doi.org/10.1016/J.MOLLIQ.2018.12.055
53. Ahmadi MH, Sadeghzadeh M, Maddah H, Solouk A, Kumar R, Chau K. Precise smart model for estimating dynamic viscosity of SiO2/ethylene glycol–water nanofluid. *Eng Appl Comput Fluid Mech*. 2019; 13: 1095-1105. https://doi.org/10.1080/19942060.2019.1668303
54. Khodadadi H, Toghraie D, Karimipour A. Effects of nanoparticles to present a statistical model for the viscosity of MgO-water nanofluid. *Powder Technol*. 2019; 342: 166-180.